

Correction to: Effect of the rotation and tidal dissipation history of stars on the evolution of close-in planets

Correction to: *Celest Mech Dyn Astr* (2016) 126:275296
<https://doi.org/10.1007/s10569-016-9690-3>

Emeline Bolmont^{1,2,3} · Stéphane Mathis²

the date of receipt and acceptance should be inserted later

Abstract This is an erratum for the publication Bolmont & Mathis 2016 (*Celestial Mechanics and Dynamical Astronomy*, 126, 275-296). There was a small mistake for the spin integration of our code which we corrected and we take advantage of this erratum to investigate a bit further the influence of a planet on the spin of its host star.

Keywords Planets and satellites: dynamical evolution and stability – Planet-star interactions – Planets and satellites: terrestrial planets – Planets and satellites: gaseous planets – stars: evolution – stars: rotation

The code used in Bolmont & Mathis (2016) had a small mistake for the spin integration. While this does not change the results of the simulations and most of the plots, the correction of this bug has an impact on Figure 5.

Figure 5 displayed the difference between the rotation period of a star with an outward-migrating planet and the rotation of the same star without planet. This Figure has the purpose of showing the impact of the planet on the rotation of its host star. The variations of the stellar rotation period induced by the migration of the planet are quite small compared to the spin-up and spin-down amplitude, plotting the difference allows to magnify and isolate this effect.

We take advantage of this erratum where we corrected our code to explain and investigate the evolution of the rotation period of a star with a migrating planet compared to the evolution of the rotation period of a star without planet. We define here δP as the difference between the rotation period of the star with planet $P_{\star, \text{pl}}$ and the rotation period of the star without planet $P_{\star, \text{no pl}}$

$$\delta P(t) = P_{\star, \text{pl}}(t) - P_{\star, \text{no pl}}(t). \quad (1)$$

Similarly we define $\delta \Omega = \Omega_{\star, \text{pl}}(t) - \Omega_{\star, \text{no pl}}(t)$ as the difference between the spin of the star with planet and the spin of the star without planet. Ω_{\star} is here the angular velocity of the star: $\Omega_{\star} = 2\pi/P_{\star}$.

Emeline Bolmont

E-mail: emeline.bolmont@unige.ch

¹ NaXys, Department of Mathematics, University of Namur, 8 Rempart de la Vierge, 5000 Namur, Belgium

² AIM, CEA, CNRS, Université Paris-Saclay, Université Paris Diderot, Sorbonne Paris Cité, F-91191 Gif-sur-Yvette, France

³ Observatoire Astronomique de l'Université de Genève, Université de Genève, Chemin des Maillettes 51, 1290 Versoix, Switzerland

The star is considered here to have a solid rotation. The planets are on coplanar and circular orbits. We remind here the Equations governing the evolution of the spin Ω_\star of the star (Equation 14 of Bolmont & Mathis 2016)

$$\begin{aligned} \frac{dI_\star \Omega_\star}{dt} = & -K \Omega_\star^\mu \omega_{\text{sat}}^{3-\mu} \left(\frac{R_\star}{R_\odot} \right)^{1/2} \left(\frac{M_\star}{M_\odot} \right)^{-1/2} \\ & + \frac{h}{2T_\star} \left[1 - \frac{\Omega_\star}{n} \right], \end{aligned} \quad (2)$$

where I_\star is the stellar moment of inertia which varies as the radius of the star R_\star evolves (we use the evolution grids of Siess et al., 2000), h the orbital angular momentum, n the mean orbital angular frequency, T_\star is the stellar dissipation timescale (see Eq. 13 of Bolmont & Mathis 2016, note that $1/T_\star \propto a^{-8}$). K , and ω_{sat} are parameters of the stellar wind model from Bouvier et al. (1997), which is valid for Main Sequence stars in the studied mass range. If $\Omega_\star > \omega_{\text{sat}}$, $\mu = 1$ and if $\Omega_\star < \omega_{\text{sat}}$, $\mu = 3$. Equation 2 becomes

$$\frac{d\Omega_\star}{dt} = \frac{1}{I_\star} \left[-\dot{I}_\star \Omega_\star - K \Omega_\star^\mu \omega_{\text{sat}}^{3-\mu} \left(\frac{R_\star}{R_\odot} \right)^{1/2} \left(\frac{M_\star}{M_\odot} \right)^{-1/2} + \frac{h}{2T_\star} \left[1 - \frac{\Omega_\star}{n} \right] \right]. \quad (3)$$

If we write this equation in terms of the stellar rotation period $P_\star = 2\pi/\Omega_\star$, we get

$$\frac{dP_\star}{dt} = \frac{-2\pi}{I_\star} \left[-\dot{I}_\star \Omega_\star^{-1} - K \Omega_\star^{\mu-2} \omega_{\text{sat}}^{3-\mu} \left(\frac{R_\star}{R_\odot} \right)^{1/2} \left(\frac{M_\star}{M_\odot} \right)^{-1/2} + \frac{h}{2T_\star \Omega_\star^2} \left[1 - \frac{\Omega_\star}{n} \right] \right]. \quad (4)$$

Let us consider an initially fast rotating Sun-like star ($M_\star = 1 M_\odot$, $P_{\star,0} = 1.2$ day). Figure 1 shows the orbital evolution of Jupiter mass planets around a Sun-like star and the evolution of the spin of the star. As in Bolmont & Mathis (2016), we consider that the initial time of our simulations is 5 Myr. The planets are distributed between an initial semi-major axis of 0.022 AU and 0.04 AU. The planets, initially outside the corotation distance, migrate outwards and therefore by conservation of angular momentum act to slow down the contraction induced spin-up of the star. $\delta\Omega$ has a straightforward evolution, the star spins down when the planet is migrating outwards. The closer the planet to the corotation distance, the farther the migration and the larger the spin-down of the star. Once the migration has stopped the winds tend to spin down faster the star which rotates faster (the star without planet), and slower the star which rotates slower (the star with planet). This leads to a convergence towards 0 of $\delta\Omega$.

However, the evolution of δP is not as straightforward. It increases as it should until an age of ~ 10 Myr, then decreases until the end of the contraction phase (where the stellar rotation is the fastest), increases significantly until ~ 500 Myr (when the star passes from a saturated regime to an unsaturated one) and then decreases towards 0.

To explain this behavior, let us consider two stars 1 and 2 of same age but different rotation periods, $P_1 = 2\pi/\Omega_1$ and $P_2 = 2\pi/\Omega_2$. As the stars have the same age, they have the same radius $R_1 = R_2 = R_\star$ and moment of inertia $I_1 = I_2 = I_\star$ (here, we neglect the impact of rotation on stellar structure and evolution; e.g. Maeder 2009 and references therein). From Equ. 4, we can compute the derivative of $\Delta P = P_1 - P_2$

$$\frac{d\Delta P}{dt} = \frac{2\pi}{I_\star} \frac{\Omega_2 - \Omega_1}{\Omega_1 \Omega_2} \times \begin{cases} \dot{I}_\star - K \Omega_1 \Omega_2 \left(\frac{R_\star}{R_\odot} \right)^{1/2} \left(\frac{M_\star}{M_\odot} \right)^{-1/2}, & \text{if } \{\Omega_1, \Omega_2\} < \omega_{\text{sat}}, \\ \dot{I}_\star + K \omega_{\text{sat}}^2 \left(\frac{R_\star}{R_\odot} \right)^{1/2} \left(\frac{M_\star}{M_\odot} \right)^{-1/2}, & \text{if } \{\Omega_1, \Omega_2\} > \omega_{\text{sat}}. \end{cases} \quad (5)$$

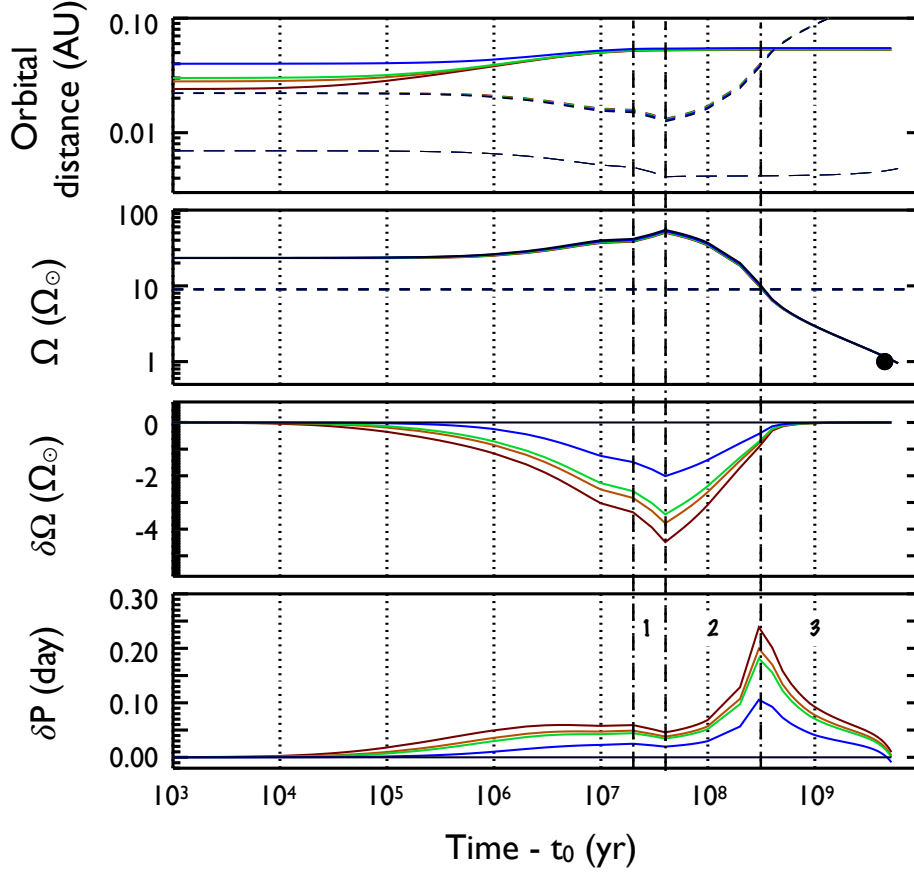


Fig. 1 Tidal evolution of Jupiter mass planets around an initially fast rotating Sun-like star. Top panel: evolution of the semi-major axis of the planet (colored full lines), corotation distance (dashed lines) and stellar radius (long dashed lines). Middle top panel: evolution of the spin of the star (full lines) and the saturation spin ω_{sat} (dashed line). The black lines correspond to the case with no planet and the present day rotation of the Sun is represented by the black dot. Middle bottom panel: evolution of $\delta\Omega$. Bottom panel: evolution of δP . Note that $\delta\Omega$ for the closest planet (in blue) also changes sign when δP does towards the end of the evolution, however the scale allowing us to display the full evolution of $\delta\Omega$ does not allow to show this sign reversal.

Let us consider that star 1 spins slower than star 2 (e.g., star 1 had an outward-migrating planet, star 2 has no planet) so that $\Omega_1 < \Omega_2$. If the two stars are in the saturated regime, then $\frac{d\Delta P}{dt}$ has the sign of $\dot{I}_\star + K\omega_{\text{sat}}^2 \left(\frac{R_\star}{R_\odot}\right)^{1/2} \left(\frac{M_\star}{M_\odot}\right)^{-1/2}$. This means that there is a critical derivative of the moment of inertia \dot{I}_{crit} defined as

$$\dot{I}_{\text{crit}} = -K\omega_{\text{sat}}^2 \left(\frac{R_\star}{R_\odot}\right)^{1/2} \left(\frac{M_\star}{M_\odot}\right)^{-1/2}. \quad (6)$$

If the two stars are in the unsaturated regime, then $\frac{d\Delta P}{dt}$ has the sign of $\dot{I}_\star - K\Omega_1\Omega_2 \left(\frac{R_\star}{R_\odot}\right)^{1/2} \left(\frac{M_\star}{M_\odot}\right)^{-1/2}$. In our example, the unsaturated regime is reached when the star is on the main sequence so

when $\dot{I}_\star \approx 0$, so that here $\frac{d\delta P}{dt}$ is negative. We can therefore identify the different phases of the evolution of $\delta P = P_1 - P_2$.

- If the stars are in the saturated regime and if $\dot{I}_\star < \dot{I}_{\text{crit}}$, which is verified if the star experiences a strong contraction (i.e. just before the main sequence, or in absolute values: $|\dot{I}_\star| > |\dot{I}_{\text{crit}}|$), δP decreases (the rotations converge): this is the phase number 1 of Fig. 1.
- If the stars are in the saturated regime and if $\dot{I}_\star > \dot{I}_{\text{crit}}$, which is verified if the stellar moment of inertia does not evolve much (i.e. during most of the PMS and the MS), δP increases (the rotations diverge). This is what happens from the end of the contraction phase (~ 50 Myr) to the unsaturated/saturated transition (~ 500 Myr): this is the phase number 2 of Fig. 1.
- If the stars are in the unsaturated regime and on the main sequence, δP decreases (the rotations converge): this is the phase number 3 of Fig. 1.
- If the stars are in the unsaturated regime and at the beginning of the giant branch (where the radius of the star increases sufficiently so that $\dot{I}_\star > K\Omega_1\Omega_2\left(\frac{R_\star}{R_\odot}\right)^{1/2}\left(\frac{M_\star}{M_\odot}\right)^{-1/2}$, δP increases (the rotations diverge). We can see this effect starting to operate as the slope of δP changes its inflection around 3 Gyr (bottom panel of Fig. 1). But this trend cannot really be seen because at late ages, the planets begin to fall towards the star making it accelerate slightly.

Figure 2 shows the evolution of Jupiter mass planets around stars of different masses, $M_\star = 0.6 M_\odot$ and $M_\star = 1.2 M_\odot$. As expected, the effect of the planet on the stellar rotation decreases as stellar mass increases. For $M_\star = 0.6 M_\odot$, the evolution is similar to the evolution for $1 M_\odot$, with a maximum of δP occurring at the transition saturated/unsaturated. For $M_\star = 1.2 M_\odot$, the star is always in the unsaturated regime so the shape is less complex. The wind is here acting to damp the effect of the planet even before the migration has finished.

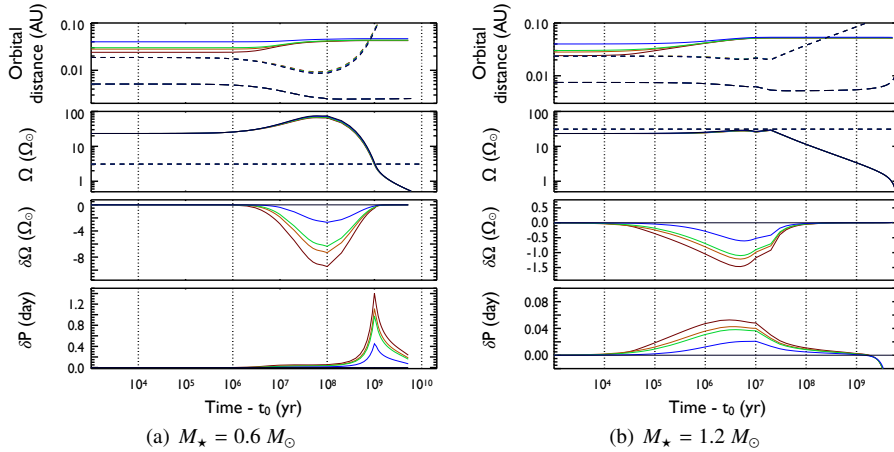


Fig. 2 Same as Fig. 1 but for different masses: (a) $0.6 M_\odot$, (b) $1.2 M_\odot$. Note that the scales are different for the two cases.

As explained in Bolmont & Mathis (2016), due to the different values of the stellar dissipation and its evolution, the migration occurs faster for the more massive star and on longer timescales for the less massive star. This means that the maximum of δP occurs earlier for the more massive star and later for the less massive star.

In order to represent the evolution of δP with the age of the star, we updated in Figure 3 the Figure 5 of Bolmont & Mathis (2016) for four different ages: at 8 Myr (around the maximum effect for the star of $1.2 M_{\odot}$), at 500 Myr (around the maximum effect for the star of $1.0 M_{\odot}$), at 1 Gyr (around the maximum effect for the star of $0.6 M_{\odot}$) and at 5 Gyr (the age used for Fig. 5 of Bolmont & Mathis 2016). We consider planet masses from the mass of Earth to five times the mass of Jupiter.

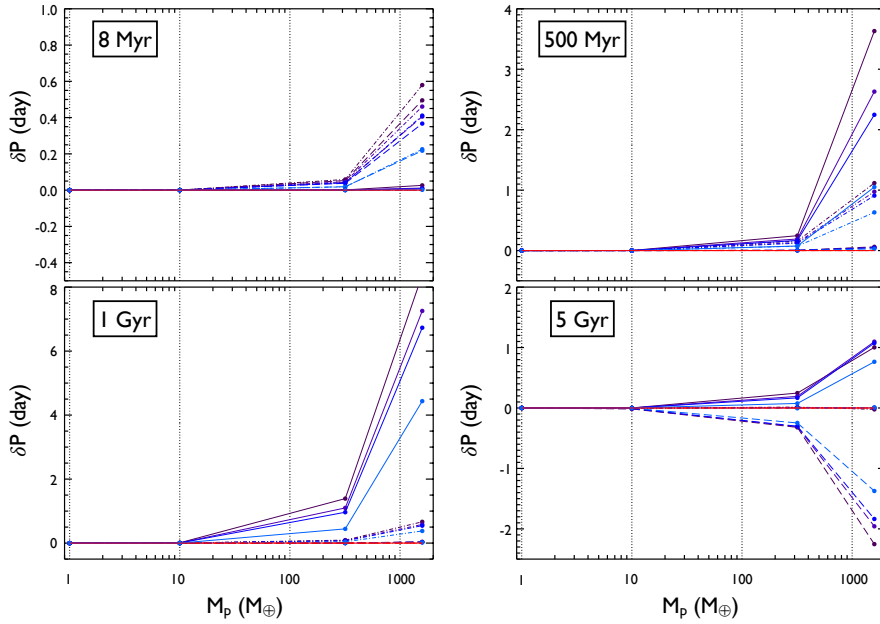


Fig. 3 δP for different initial orbital distances and for the 3 different stars and 4 different ages. The solid lines correspond to the $0.6 M_{\odot}$ star, the dashed-dotted lines correspond to $1.0 M_{\odot}$ and the long-dashed lines correspond to $1.2 M_{\odot}$. From purple to light blue: an initial semi-major axis of 0.024, 0.028, 0.030 and 0.040 AU. The red line marks $\delta P = 0$ day. Note that the scales are different for each panel.

The effect of the planet on the star is much less pronounced than what was shown on Figure 5 of Bolmont & Mathis (2016). The effect of a Jupiter mass planet on the rotation of a $0.6 M_{\odot}$ star is of 0.1 to 0.3 days at 5 Gyr, while Bolmont & Mathis (2016) was showing an effect of 2.2 to 3 days. Note also that for the $1.2 M_{\odot}$ star, the stars with planets rotate faster than the star without planets. This coincides with the beginning of the red giant branch when the radius of the star starts to increase (see Fig. 2(b)) and the planets have already started to migrate inwards.

However, the planet can still have quite an important impact on the rotation towards the end of the outward migration. This is thus an effect which highly depends on the age of the

star, and which could eventually be observable via high-precision photometry (McQuillan et al., 2013; García et al., 2014; Ceillier et al., 2016).

Acknowledgements The authors would like to thank the anonymous referee for his comments on this manuscript. E. B. and S. M. acknowledge funding by the European Research Council through ERC grant SPIRE 647383.

References

- Bolmont, E. & Mathis, S. 2016, *Celestial Mechanics and Dynamical Astronomy*, 126, 275
Bouvier, J., Forestini, M., & Allain, S. 1997, *A&A*, 326, 1023
Ceillier, T., van Saders, J., García, R. A., et al. 2016, *MNRAS*, 456, 119
García, R. A., Ceillier, T., Salabert, D., et al. 2014, *A&A*, 572, A34
Maeder, A. 2009. *Physics, Formation and Evolution of Rotating Stars*. Springer Berlin Heidelberg.
McQuillan, A., Mazeh, T., & Aigrain, S. 2013, *ApJ*, 775, L11
Siess, L., Dufour, E., & Forestini, M. 2000, *A&A*, 358, 593